

Chaos synchronization in a BEC system using fuzzy logic controller

E. Tosityali ¹, *Y. Oniz ², F. Aydogmus ³

¹ Opticianry, Vocational School of Health Services, Istanbul Bilgi University, Kustepe, Sisli, Istanbul, 34387, Turkey

² Faculty of Engineering and Natural Sciences, Department of Mechatronics Engineering, Istanbul Bilgi University, Eyup, Istanbul, 34060, Turkey

³ Faculty of Science, Physics, Istanbul University, Vezneciler, Istanbul, 34134, Turkey

Received April 13, 2022, in final form August 31, 2022

Since the presence of chaos in Bose-Einstein condensate (BEC) systems plays a destructive role that can undermine the stability of the condensates, controlling the chaos is of great importance for the creation of the BEC. In this paper, a fuzzy logic controller (FLC) to synchronize the chaotic dynamics of two identical master-slave BEC systems has been proposed. Unlike the conventional approaches, where expert knowledge is directly used to construct the fuzzy rules and membership functions, the fuzzy rules have been constructed using Lyapunov stability theorem ensuring the synchronization process. The effectiveness of the proposed controller has been demonstrated numerically.

Key words: *fuzzy logic controller, synchronization, chaos, Bose-Einstein condensate*

1. Introduction

Bose-Einstein condensation (BEC) is a process, in which the system forms a single coherent matter wave after the temperature of boson gases is reduced below a critical level. The theoretical background of BEC was set by Einstein in [1, 2], with the idea that the boson gases will experience a phase transition at their critical temperature, whereas the idea was experimentally verified in 1995 using the dilute atomic vapor of rubidium and sodium [3, 4].

Despite the fact that the temperatures obtained with lasers are quite low, to be able to form BEC, an additional cooling method is required to enable the atoms with relatively higher energy to escape from the trap [5]. In this cooling method, which reduces the kinetic energy of the entire system, the magneto-optical trap and lasers are turned off while another magnetic field is activated at the same time. The energy of the atoms at the center of the trap is considerably smaller than the energy of the atoms at the corners of the trap. Trapped dilute boson gases interact with each other due to their physical properties or due to collisions. In the interacting gases, only weakly interacting states caused by binary collisions (*s*-wave scattering) are considered, as it is not possible to express the system macroscopically with a single wave function in non-weak interactions.

Radiofrequency is used to enable atoms with higher energies to escape from the trap, which provides a change in the spinning direction of the atoms. This process generates a repulsive force for atoms, where the magnetic field and the magnetic moment are parallel. An attractive force occurs among the atoms due to opposite magnetic moments. The repulsive force separates the atomic cloud as trapped and untrapped, and allows the atoms with more energy standing at the corners to be thrown out of the trap. The atoms in the trap collide and transfer their momentum to each other; and they come into equilibrium at a new low thermal energy called back thermalization. This process is repeated until the critical temperature is reached [6].

*Corresponding author: eren.tosityali@bilgi.edu.tr.

The condensation of weakly interacting boson gases, for which the temperature is close to zero, is well expressed by the Gross-Pitaevskii equation (GPE). This equation was derived in 1961 by Gross and Pitaevskii independently and with different techniques to describe weakly interacting dilute boson gases [7, 8]. Basically, the GPE is the nonlinear Schrödinger equation derived from mean-field theory. The GPE gives favorable results in the experiments with weakly interacting BEC.

It is of great importance to study how to control the chaos of a BEC system in an optical lattice which exhibits many rich and complex phenomena typical of nonlinear systems [9–13]. An important approach to consider is the synchronization problem from a control theory perspective.

Different control schemes including feedback control [14–17], sliding mode control, [18, 19] and fuzzy logic control [20, 21] have been proposed over the last decade for the synchronization problem of chaotic systems. The main drawback of the feedback control schemes is that the control signals are generated relying on the mathematical model of the chaotic system. However, in many applications the dynamics of the system will be perturbed because of the uncertainties in the system parameters and external disturbances. Hence, these controllers may fail to provide reliable results. The sliding mode control approach can be pointed out among the most effective robust controllers to handle high-order nonlinear systems. However, this approach inherently suffers from the chattering problem. On the other hand, fuzzy logic controllers (FLC) provide an easy but effective way to cope with uncertain and nonlinear system dynamics, and they were successfully applied in many areas such as control [22, 23], decision making [24, 25], prediction [26, 27], forecasting [28, 29], and modelling [30, 31]. Recently, fuzzy logic control of chaotic systems has become an active research area. In the fuzzy logic control, the output of the controller is determined using the fuzzy inference. The rules typically rely on expert knowledge. Although promising results have been reported in the literature for the use of this conventional scheme in chaos synchronization [32, 33], the performance of these controllers might significantly degrade if expert knowledge is incomplete and/or uncertain. To alleviate this issue, adaptive approaches are commonly preferred in the design of FLCs, in which the controller parameters are updated to lead the synchronization error to zero [34, 35]. Despite the fact that the adaptive schemes can provide fairly good results, their time requirements for the adaptation process might pose a problem in real-time applications. In the proposed work, the Lyapunov stability theorem was directly employed to construct the consequent part of the fuzzy rules such that two identical master-slave BEC systems can be synchronized. One of the most prominent advantages of this control scheme is that the stability in the Lyapunov sense of error dynamics of two identical chaotic BEC motions was ensured. The feasibility and effectiveness of the proposed controller were demonstrated by numerical simulation results.

2. Description of system

GPE including macroscopic wave function can well describe the evolution of the BEC simultaneously with regard to time and space [7, 8]. One-dimensional (1D) GPE can be described as below:

$$i\hbar \frac{\partial}{\partial t} \Psi(x, t) = -\frac{\hbar^2}{2m} \frac{\partial^2}{\partial x^2} \Psi(x, t) + [V_{\text{ext}}(x) + g_{1D} |\Psi(x, t)|^2] \Psi(x, t), \quad (2.1)$$

where m stands for the mass of the atoms which constitute the BEC, V_{ext} is the external potential with tilted term trapping from the BEC, and g_{1D} is the one dimensional interaction term between the atoms defined as:

$$g_{1D} = \frac{g_{3D}}{2\pi a_r^2} = 2a_s \hbar \omega_r,$$

with a_s being the s -wave scattering length between atoms. s -wave scattering length could be positive or negative depending on the interactions whether it is repulsive or attractive, respectively. In our case, its value is negative due to attractive interactions. ω_r is the ground state of a harmonic frequency of the oscillator.

The external trap potential $V_{\text{ext}}(x)$ is given as:

$$V_{\text{ext}}(x) = V_1 \cos^2(\omega_1 x) + V_2 \cos^2(\omega_2 x) + Fx. \quad (2.2)$$

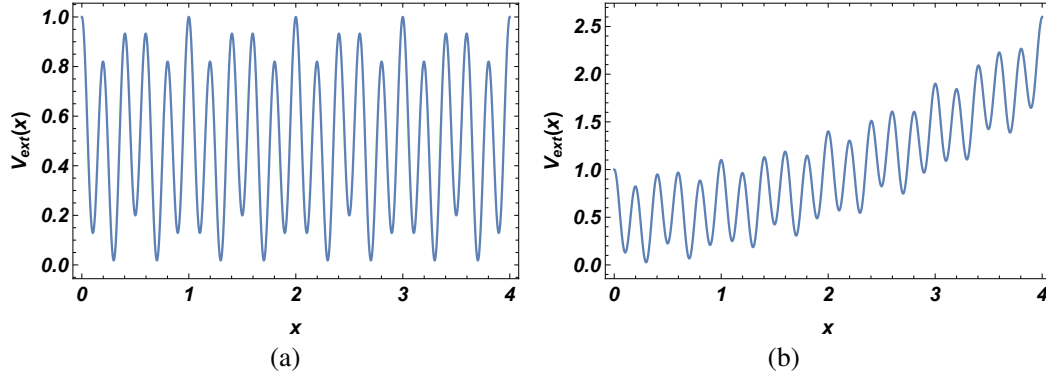


Figure 1. (Colour online) Plot of the bichromatic optical lattice potential with the parameters $\nu_1 = 1$, $\nu_2 = 0.8$, $\omega_1 = 2\pi$, $\omega_2 = 5\pi$, (a) $F = 0$, (b) $F = 0.1$.

V_{ext} comprises two parts: while the first part of double well potential with two frequencies is related to the optical lattice potential, the second part is related to the tilted potential. Here, V_1 and V_2 are the amplitudes, F is the internal force and Fx corresponds to the tilted potential, which makes the atoms tunnelling out from the potential and accelerates them in the x direction. 1D Hamiltonian ($H_F = H_0 + Fx$) tends to infinity when $|x| \rightarrow \infty$ [36]. However, the Hamiltonian is always bounded if the lattice size is finite $-L \leq x \leq L$ [37]. The BEC system of this study is bounded with 100 lattice sites. The number of lattice sites was determined empirically as 100, which implies that $L \sim 100\pi k^{-1}$ ($k = 2\pi/850 \text{ nm}^{-1}$) [38–40]. To meet the requirements on the numbers of the lattice sites and thus on the boundary conditions, the simulated studies were carried out for 1000 steps with a step size of 0.1, and for 10000 steps with a step size of 0.01. In figure 1, the evolution of the external potential for parameters set $\nu_1 = 1$, $\nu_2 = 0.8$, $\omega_1 = 2\pi$, $\omega_2 = 5\pi$, (a) $F = 0$, (b) $F = 0.1$ is illustrated.

There are different time-dependent ansatzs to solve the GPE [41, 42]. In this study, the following widely-used form of the time-dependent wave function is preferred:

$$\Psi(x, t) = \Phi(x) e^{-i\mu t/\hbar}, \quad (2.3)$$

here, μ is the chemical potential of the condensate and $\Phi(x)$ is a real function independent of time. Normalized $\Phi(x)$ gives the total number of particles in the system, i.e.,

$$\int |\Phi(x)|^2 dx = N, \quad (2.4)$$

where N is the particle number. Substitution of equations (2.2) and (2.3) into equation (2.1) yields:

$$\mu\Phi(x) = -\frac{\hbar^2}{2m} \frac{d^2}{dx^2} \Phi(x) + [V_1 \cos^2(\omega_1 x) + V_2 \cos^2(\omega_2 x) + Fx + g_{1D} |\Phi(x)|^2] \Phi(x). \quad (2.5)$$

Using the dimensionless parameters $\nu_1 = 2mV_1/\hbar^2$, $\nu_2 = 2mV_2/\hbar^2$, $\gamma = 2m\mu/\hbar^2$, $\eta = 2mg_0/\hbar^2$, $\Gamma = 2mF/\hbar^2$, the equation (2.5) can be written as:

$$\frac{d^2\Phi}{dx^2} = [\nu_1 \cos^2(\omega_1 x) + \nu_2 \cos^2(\omega_2 x) + \Gamma x - \gamma + \eta |\Phi|^2] \Phi. \quad (2.6)$$

The solution of equation (2.6) has the following form:

$$\Phi(x) = \phi(x) e^{i\theta(x)}, \quad (2.7)$$

where ϕ and θ are real functions of x , expressing the amplitude and the phase, respectively. The first derivative of the phase is proportional to the velocity field, and the squared amplitude corresponds to

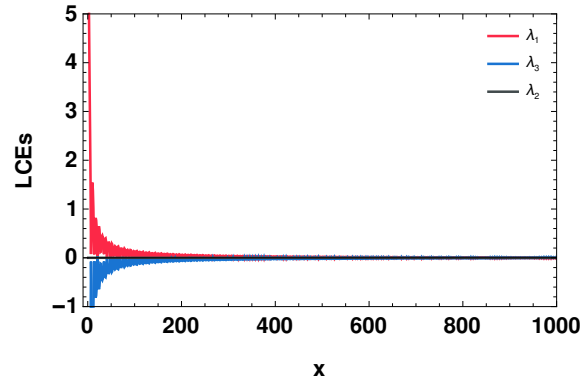


Figure 2. (Colour online) LCEs for paramter sets: $J = 0.4$, $\nu_1 = 1$, $\nu_2 = 0.8$, $\omega_1 = 2\pi$, $\omega_2 = 5\pi$, $\Gamma = 0.1$, $\eta = -0.015$, $\gamma = 0.5$ and initial condition: $(x_1 = 1, y_1 = -1)$.

the density of the atoms in the condensate. Substituting equation (2.7) into equation (2.6) results in two coupled equations, which correspond to the real and imaginary parts.

$$\frac{d^2\phi}{dx^2} = \phi \left(\frac{d\theta}{dx} \right)^2 + [\nu_1 \cos^2(\omega_1 x) + \nu_2 \cos^2(\omega_2 x) + \Gamma x - \gamma + \eta |\phi|^2] \phi, \quad (2.8)$$

$$\frac{d^2\theta}{dx^2} + 2 \frac{1}{\phi} \frac{d\theta}{dx} \frac{d\phi}{dx} = 0. \quad (2.9)$$

Integration of equation (2.9) gives the relation between the velocity field and the particle number density,

$$J = 2\phi^2 \left(\frac{d\theta}{dx} \right), \quad (2.10)$$

where J represents the steady super-fluidity phase in fluid dynamics. Using J in equation (2.8), the following nonlinear equation can be obtained:

$$\frac{d^2\phi}{dx^2} = \frac{J^2}{4\phi^3} + [\nu_1 \cos^2(\omega_1 x) + \nu_2 \cos^2(\omega_2 x) + \Gamma x - \gamma + \eta |\phi|^2] \phi. \quad (2.11)$$

The equation (2.11) was solved numerically for 1000 steps with 100 eliminated steps, with a step size of 0.1 to satisfy the 100 lattice site boundary condition. In the simulation, the following values for the parameters were assumed: $J = 0.4$, $\nu_1 = 1$, $\nu_2 = 0.8$, $\omega_1 = 2\pi$, $\omega_2 = 5\pi$, $\Gamma = 0.1$, $\eta = -0.015$, $\gamma = 0.5$ and possible initial conditions $(x_1 = 1, y_1 = -1)$ by the Runge-Kutta method. The Lyapunov characteristic exponents (LCEs) of the BEC system given in figure 2 are $\lambda_1 = 0.0046543$, $\lambda_2 = 0$ and $\lambda_3 = -0.00465435$. For the given system parameters and initial conditions, the system exhibits chaotic behaviour due to the presence of positive LCE.

Using the transformations $d\phi/dx = dx_1/dx$ and $d^2\phi/dx^2 = dy_1/dx$, the equation (2.11) can be re-written with the following first-order coupled equations, which defines the master system as:

$$\frac{dx_1}{dx} = y_1, \quad (2.12)$$

$$\frac{dy_1}{dx} = \frac{J^2}{4x_1^3} + [\nu_1 \cos^2(\omega_1 x) + \nu_2 \cos^2(\omega_2 x) + \Gamma x - \gamma + \eta |x_1|^2] x_1, \quad (2.13)$$

and the dynamics of the slave system are given below:

$$\frac{dx_2}{dx} = y_2. \quad (2.14)$$

$$\frac{dy_2}{dx} = \frac{J^2}{4x_2^3} + [v_1 \cos^2(\omega_1 x) + v_2 \cos^2(\omega_2 x) + \Gamma x - \gamma + \eta |x_2|^2] x_2 + \Delta f(x_2, y_2) + u(x), \quad (2.15)$$

where u is the control input, $\Delta f(x_2, y_2)$ is the uncertain term which is assumed bounded, i.e., $\Delta f(x_2, y_2) \leq \alpha$, where α is a positive constant. It is also assumed that $\Delta f(x_2, y_2)$ satisfy all the necessary conditions, such as system (2.14), (2.15) having a unique solution in the spatial evolution $x_0 + \infty$, for any given initial condition. In this paper, the control input $u(x)$ is derived to synchronize the master and slave system.

3. Fuzzy design for chaotic synchronization

Fuzzy inference can be defined as a process, in which the given input(s) are mapped to the output(s) using the fuzzy set theory. Figure 3 depicts the general structure of a fuzzy inference system, which consists of four main function blocks:

1. The knowledge base comprises expert knowledge and it can be separated into two parts: database and rule base. In the database, the type and parameters of the membership functions are stored, whereas the rule base includes the fuzzy “if-then” rules.
2. In the fuzzification stage, the crisp input variables are transformed into fuzzy sets using the expert knowledge stored in the database. Hence, the outputs of this block are fuzzy sets.
3. In the inference engine, using the fuzzy “if-then” rules stored in the rule base, rule consequents are computed for each rule and aggregated into a single fuzzy output set.
4. Output fuzzy sets are transformed into crisp output values in the defuzzification step.

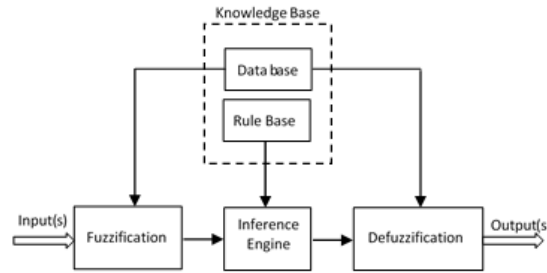


Figure 3. Structure of a fuzzy inference system.

In order to synchronize the master and slave system with the dynamics given in equations (2.12)–(2.15), the error states are defined as $e_1 = x_2 - x_1$ and $e_2 = y_2 - y_1$ by subtracting the master system from the slave system. The error dynamics can be specified as:

$$\frac{de_1}{dx} = e_2, \quad (3.1)$$

$$\frac{de_2}{dx} = [v_1 \cos^2(\omega_1 x) + v_2 \cos^2(\omega_2 x) + \Gamma x - \gamma] e_1 + \Delta f(x_2, y_2) + u_L. \quad (3.2)$$

The control input $u(x)$ in equation (2.15) can be written as $u(x) = u_{eq} + u_L$, where $u_{eq} = -\eta |x_2|^2 x_2 + \eta |x_1|^2 x_1$. A fuzzy logic controller is proposed to construct the control input u_L , where the error dynamics in equation (3.1) and (3.2) are utilized as the input signals of the FLC. These incoming signals, (e_1, e_2) , are fuzzified using triangular membership functions shown in figure 4, and associated with A_i and B_j fuzzy subsets, respectively, which are defined by their corresponding membership functions $\mu_{A_i}(e_1)$ and $\mu_{B_j}(e_2)$ for $i = 1, \dots, I$ and $j = 1, \dots, J$.

The fuzzy “if-then” rule R_{ij} with the inputs (e_1, e_2) and the output u_L can be stated as:

Table 1. Rule Table of FLC.

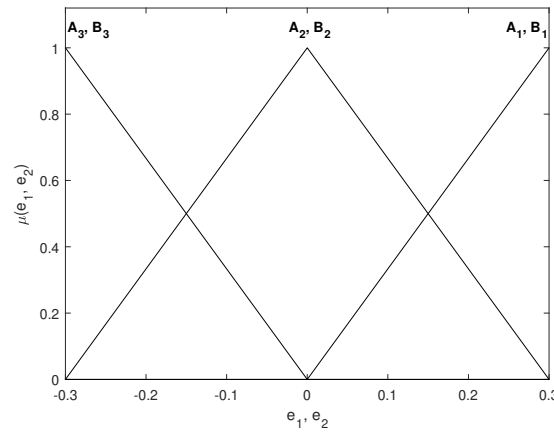
| Rule | Antecedent | | Consequent |
|------|------------|-------|------------|
| | e_1 | e_2 | |
| 1 | A_1 | B_1 | $u_{L,11}$ |
| 2 | A_1 | B_2 | $u_{L,12}$ |
| 3 | A_1 | B_3 | $u_{L,13}$ |
| 4 | A_2 | B_1 | $u_{L,21}$ |
| 5 | A_2 | B_2 | $u_{L,22}$ |
| 6 | A_2 | B_3 | $u_{L,23}$ |
| 7 | A_3 | B_1 | $u_{L,31}$ |
| 8 | A_3 | B_2 | $u_{L,32}$ |
| 9 | A_3 | B_3 | $u_{L,33}$ |

R_{ij} : If e_1 is A_i and e_2 is B_j , then $u_L = u_{L,ij}(e_1, e_2)$,

where $u_{L,ij}$ is an analytical function of e_1, e_2 that stabilizes the error dynamics in equation (3.1) and (3.2). Minimum t-norm is employed to calculate the firing strengths of each rule, i.e., $W_{ij} = \min[\mu_{A_i}(e_1), \mu_{B_j}(e_2)]$, whereas the centroid defuzzification method is used to compute the output control signal u_L :

$$u_L = \frac{\sum_{i=1}^I \sum_{j=1}^J W_{ij} u_{L,ij}}{\sum_{i=1}^I \sum_{j=1}^J W_{ij}}. \quad (3.3)$$

The fuzzy rules used in this study are presented in table 1, in which e_1 and e_2 correspond to the input variables used in the antecedent part of the rules, and $u_{L,ij}$ denotes the output variable of the consequent. As illustrated in figure 4, three membership functions are used for each input: A_1, A_2 and A_3 for the input signal e_1 , and B_1, B_2 and B_3 for the input signal e_2 . The membership functions $\{A_1, B_1\}$, $\{A_2, B_2\}$ and $\{A_3, B_3\}$ correspond to positive, zero and negative error dynamics, respectively.

**Figure 4.** Membership functions.

The following function, which is positive and continuously differentiable, is selected as the Lyapunov function candidate:

$$V = \frac{1}{2} (e_1^2 + e_2^2). \quad (3.4)$$

To ensure the Lyapunov stability, the following condition should be met [43]:

$$\dot{V} = e_1 \dot{e}_1 + e_2 \dot{e}_2 < 0, \quad (3.5)$$

which requires $\dot{e}_2 < -e_1/e_2$. For the following cases, the consequents of the FLC are proposed such that the stability condition is ensured.

Case 1: $e_2 < 0$

For $e_2 < 0$, the stability condition requires that:

$$\dot{e}_2 > -e_1. \quad (3.6)$$

Substituting equation (3.6) into equation (3.1) and (3.2) produces

$$\left[v_1 \cos^2(\omega_1 x) + v_2 \cos^2(\omega_2 x) + \Gamma x - \gamma \right] e_1 + \Delta f + u_L > -e_1, \quad (3.7)$$

then $-\left[v_1 \cos^2(\omega_1 x) + v_2 \cos^2(\omega_2 x) + \Gamma x - \gamma - 1 \right] e_1 - \Delta f < u_L$ should be provided. Assuming that the uncertainty term Δf is bounded, that is $|\Delta f| \leq \alpha$, with α being a positive constant, the following equality can be derived:

$$-\left[v_1 \cos^2(\omega_1 x) + v_2 \cos^2(\omega_2 x) + \Gamma x - \gamma + 1 \right] e_1 + \alpha = u_1^*. \quad (3.8)$$

Case 2: $e_2 > 0$

If $e_2 > 0$, then:

$$\dot{e}_2 < -e_1, \quad (3.9)$$

should be provided to meet the stability condition. Substituting equation (3.9) into equation (3.1) and (3.2) results in:

$$\left[v_1 \cos^2(\omega_1 x) + v_2 \cos^2(\omega_2 x) + \Gamma x - \gamma \right] e_1 + \Delta f + u_L < -e_1. \quad (3.10)$$

Hence, the control input u_L should satisfy the following inequality:

$$-\left[v_1 \cos^2(\omega_1 x) + v_2 \cos^2(\omega_2 x) + \Gamma x - \gamma - 1 \right] e_1 - \Delta f > u_L. \quad (3.11)$$

A new term u_2^* can be derived as:

$$-\left[v_1 \cos^2(\omega_1 x) + v_2 \cos^2(\omega_2 x) + \Gamma x - \gamma + 1 \right] e_1 - \alpha = u_2^*. \quad (3.12)$$

According to table 1, e_2 is negative for Rules 3, 6 and 9, which corresponds to the above mentioned **Case 1**. If the terms in the consequent parts of these rules are selected as $u_1^* = u_{L,13} = u_{L,23} = u_{L,33}$, then the stability condition will be satisfied, i.e., $\dot{V} < 0$, and the error states will be asymptotically driven to zero. Similarly, for Rules 1, 4 and 7, e_2 is positive, which corresponds to **Case 2**. Hence, if the consequent parameters of these rules are selected as $u_2^* = u_{L,11} = u_{L,21} = u_{L,31}$, then the stability can be ensured.

Case 3: $e_1 > 0$ and $e_2 \in 0$

In table 1 for Rule 2, e_1 is positive, whereas e_2 is zero. To satisfy the Lyapunov stability condition stated in equation (3.5), the following equality should be provided:

$$e_1 + \dot{e}_2 = -\text{sgn}(e_2), \quad (3.13)$$

where

$$\text{sgn}(e_2) = \begin{cases} 1 : e_2 > 0, \\ -1 : e_2 < 0. \end{cases}$$

As e_1 is positive, then

$$\dot{e}_2 < -\text{sgn}(e_2), \quad (3.14)$$

should be satisfied. Substituting equation (3.14) into equation (3.1) and (3.2) yields

$$\left[v_1 \cos^2(\omega_1 x) + v_2 \cos^2(\omega_2 x) + \Gamma x - \gamma \right] e_1 + \Delta f + u_L < -\text{sgn}(e_2). \quad (3.15)$$

The equation can be written as

$$u_L < -\text{sgn}(e_2) - \left[v_1 \cos^2(\omega_1 x) + v_2 \cos^2(\omega_2 x) + \Gamma x - \gamma \right] e_1 - \Delta f, \quad (3.16)$$

which implies that if $u_{L,12}$ is selected as:

$$u_{L,12} = -\text{sgn}(e_2) - [v_1 \cos^2(\omega_1 x) + v_2 \cos^2(\omega_2 x) + \Gamma x - \gamma] e_1 - \alpha, \quad (3.17)$$

then it will satisfy the stability condition.

Case 4: $e_1 < 0$ and $e_2 \in 0$

The controller $u_{L,32}$ in Rule 8 can be derived in a way similar to Rule 2, which requires:

$$\dot{e}_2 > -\text{sgn}(e_2). \quad (3.18)$$

Substituting equation (3.18) into equation (3.1) and (3.2) yields

$$[v_1 \cos^2(\omega_1 x) + v_2 \cos^2(\omega_2 x) + \Gamma x - \gamma] e_1 + \Delta f + u_L > -\text{sgn}(e_2). \quad (3.19)$$

The equation can be written as

$$u_L > -\text{sgn}(e_2) - [v_1 \cos^2(\omega_1 x) + v_2 \cos^2(\omega_2 x) + \Gamma x - \gamma] e_1 - \Delta f. \quad (3.20)$$

To ensure the stability, the controller $u_{L,32}$ should be selected as:

$$u_{L,32} = -\text{sgn}(e_2) - [v_1 \cos^2(\omega_1 x) + v_2 \cos^2(\omega_2 x) + \Gamma x - \gamma] e_1 + \alpha. \quad (3.21)$$

Case 5: $e_1 \in 0$ and $e_2 \in 0$

For Rule 5 in Table 1, the error states e_1 and e_2 are both zero. Therefore, $u_{L,22} = 0$.

The control function of $u_{L,ij}$ with $i = 1, 2, 3$ and $j = 1, 2, 3$ depending on e_1, e_2 is summarized below. The controller parameters are derived such that all of the rules in the FLC can lead to Lyapunov stable subsystems under the same Lyapunov function (3.4). Therefore, it is ensured that the chaotic master and slave system will be synchronized.

$$\begin{aligned} u_{L,11} &= u_{L,21} = u_{L,31} = -[v_1 \cos^2(\omega_1 x) + v_2 \cos^2(\omega_2 x) + \Gamma x - \gamma + 1] e_1 - \alpha, \\ u_{L,13} &= u_{L,23} = u_{L,33} = -[v_1 \cos^2(\omega_1 x) + v_2 \cos^2(\omega_2 x) + \Gamma x - \gamma + 1] e_1 + \alpha, \\ u_{L,12} &= -\text{sgn}(e_2) - [v_1 \cos^2(\omega_1 x) + v_2 \cos^2(\omega_2 x) + \Gamma x - \gamma] e_1 - \alpha, \\ u_{L,32} &= -\text{sgn}(e_2) - [v_1 \cos^2(\omega_1 x) + v_2 \cos^2(\omega_2 x) + \Gamma x - \gamma] e_1 + \alpha, \\ u_{L,22} &= 0. \end{aligned} \quad (3.22)$$

4. Simulations and results

In this section, the FLC is applied to synchronize the two identical master and slave BEC systems of the form (2.12), (2.13) and (2.14), (2.15). For this purpose, the equation systems are solved numerically by using fourth order Runge-Kutta method. The same parameter sets are used in both master and slave system as $J = 0.4$, $v_1 = 1$, $v_2 = 0.8$, $\omega_1 = 2\pi$, $\omega_2 = 5\pi$, $\Gamma = 0.1$, $\eta = -0.015$, $\gamma = 0.5$. Initial conditions are selected as $(x_1(0), y_1(0)) = (1, -1)$ and $(x_2(0), y_2(0)) = (0.2, 0.3)$ for master and slave systems, respectively. The system is evaluated for 10000 steps with a step size of 0.01 which fulfills the 1D 100 lattice sites boundary condition. Spatial evaluation and phase space displays for master and slave BEC systems are given in Figure 5 and 6, respectively. To observe the effectiveness of the proposed control scheme more clearly, for the first 250 steps, the control input of the fuzzy logic controller, u_L , is set to zero, such that the master and slave systems are not synchronized. Following the 250th step, the computed value of u_L is directly fed to the system, which leads the error states e_1 and e_2 , to converge to zero exponentially. Thus, it can be concluded that two identical BEC systems are synchronized along the flow. The results of error states are given in figure 7, which are compatible with spatial evolution and the phase space results given in figure 5 and 6, respectively. Finally, the graph of the control input u_L is given in figure 8, from which it can be inferred that u_L is zero until $x = 250$, and it is computed with regard to equation (3.22) only after this step.

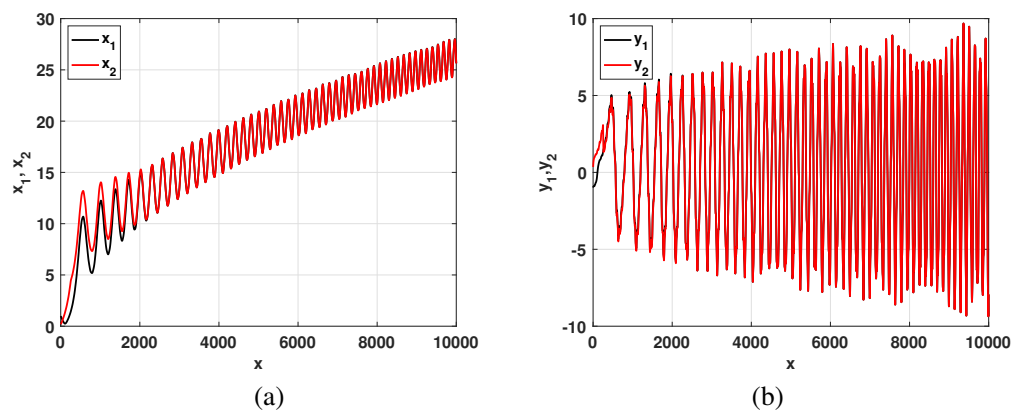


Figure 5. (Colour online) Master and slave system synchronization for chaotic BEC systems: (a) system outputs x_1 and x_2 , (b) system outputs y_1 and y_2 .

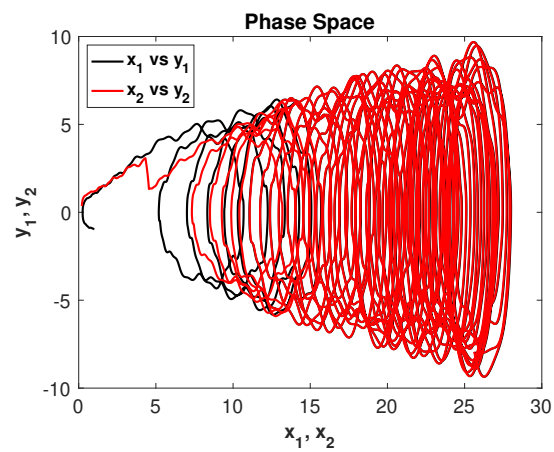


Figure 6. (Colour online) Synchronized phase space of the master and slave systems.

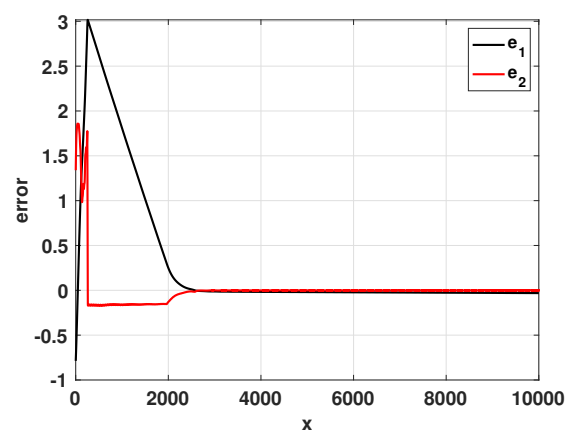


Figure 7. (Colour online) Error states for master and slave systems.

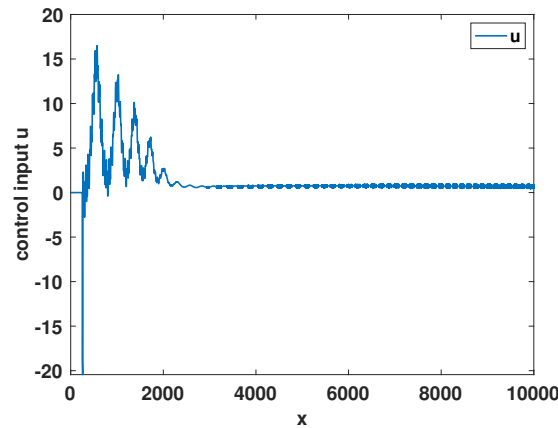


Figure 8. (Colour online) The evolution of control input u depending on x .

5. Conclusion

In this paper, the effectiveness of the fuzzy logic controller method to synchronize chaotic BEC systems is theoretically and numerically demonstrated. The chaotic synchronization system consists of the master and slave systems. In the master slave scheme, the given BEC system is considered as a master system, and the other identical BEC system is considered as a slave system. The difference between the states of the master and slave system and its derivative is selected as the input signals for the fuzzy logic controller. The consequent part of the fuzzy rules, which consists of analytical functions of the error and its derivative, is determined using the Lyapunov stability theorem to ensure the stability of the synchronization process. Furthermore, this way the dependence of the algorithm on the completeness and accuracy of the expert knowledge is also overcome. In addition, the numerical simulation results show that the error dynamics of the identical chaotic BEC synchronization systems are regulated to zero asymptotically in shorter time in spite of the overall system undergoing irregularity.

The chaos which has a destructive role for BEC could disrupt the stability in the condensate. Therefore, controlling the chaos is of great importance for the creation of BEC. A distinguishing feature of the present work is the first synchronization of the identical chaotic Bose-Einstein condensate held in a 1D tilted bichromatical optical lattice potential by using the fuzzy logic control technique. Consequently, this study will make a significant contribution in this field.

References

1. Bose S., Z. Phys., 1924, **26**, 178–181, doi:10.1007/BF01327326.
2. Einstein A., In: Akademie-Vorträge. Sitzungsberichte der Preußischen Akademie der Wissenschaften 1914–1932, Simon D. (Ed.), 2005, 245–257.
3. Anderson M. H., Ensher J. R., Matthews M. R., Wieman C. E., Cornell E. A., Science, 1995, **269**, No. 5221, 198–201, doi:10.1126/science.269.5221.198.
4. Davis K. B., Mewes M. O., Andrews M. R., van Druten N. J., Durfee D. S., Kurn D. M., Ketterle W., Phys. Rev. Lett., 1995, **75**, 3969–3973, doi:10.1103/PhysRevLett.75.3969.
5. Ketterle W., Van Druten N. J., Adv. At. Mol. Opt. Phys., 1996, **37**, 181–236, doi:10.1016/S1049-250X(08)60101-9.
6. Ensher J. R., Jin D. S., Matthews M. R., Wieman C. E., Cornell E. A., Phys. Rev. Lett., 1996, **77**, 4984–4987, doi:10.1103/PhysRevLett.77.4984.
7. Gross E. P., Phys. Rev. Lett., 1961, **20**, 454–477, doi:10.1007/BF02731494.
8. Pitaevskii L., Stringari S., Bose-Einstein Condensation, Clarendon Press, Oxford, 2003.
9. Tosyali E., Aydogmus F., Yilmaz A., Int. J. Mod. Phys. B, 2018, **32**, No. 23, 1850254, doi:10.1142/S0217979218502545.
10. Tosyali E., Fluctuation Noise Lett., 2018, **17**, No. 03, 1850027, doi:10.1142/S021947751850027X.

11. Tosityali E., Aydogmus F., *Condens. Matter Phys.*, 2020, **23**, No. 1, 13001, doi:10.5488/CMP.23.13001.
12. Tosityali E., Aydogmus F., *J. Phys.: Conf. Ser.*, 2018, **1141**, No. 1, 012124, doi:10.1088/1742-6596/1141/1/012124.
13. Aydogmus F., Tosityali E., *Int. J. Control*, 2022, **95**, No. 3, 620–625, doi:10.1080/00207179.2020.1808244.
14. Idowu B. A., Vincent U. E., *J. Chaos*, 2013, **2013**, 723581, doi:10.1155/2013/723581.
15. Guo R., *Nonlinear Dyn.*, 2017, **90**, 53–64, doi:10.1007/s11071-017-3645-4.
16. Mobayen S., Tchier F., *Asian J. Control*, 2018, **20**, No. 1, 71–85, doi:10.1002/asjc.1512.
17. Zhang Z. Y., Feng X. Q., Yao Z. H., Jia H. Y., *Chin. Phys. B*, 2015, **24**, No. 11, 110503, doi:10.1088/1674-1056/24/11/110503.
18. Chen D., Zhang R., Ma X., Liu S., *Nonlinear Dyn.*, 2012, **69**, 35–55, doi:10.1007/s11071-011-0244-7.
19. Vaidyanathan S., Azar A.T., In: *Advances and Applications in Sliding Mode Control systems. Studies in Computational Intelligence*, Vol. 576, Azar A., Zhu Q. (Eds.), Springer, Cham., 2015, 549–569, doi:10.1007/978-3-319-11173-5_20.
20. Yau H. T., Shieh C. S., *Nonlinear Anal. Real World Appl.*, 2008, **9**, No. 4, 1800–1810, doi:10.1016/j.nonrwa.2007.05.009.
21. Vaidyanathan S., Azar A. T., *Int. J. Intell. Eng. Inf.*, 2016, **4**, No. 2, 135–150, doi:10.1504/IJIEI.2016.076699.
22. Topalov A. V., Oniz Y., Kayacan E., Kaynak O., *Neurocomputing*, 2011, **74**, No. 11, 1883–1893, doi:10.1016/j.neucom.2010.07.035.
23. Khanesar M. A., Oniz Y., Kaynak O., Gao H., *IEEE/ASME Trans. Mechatron.*, 2016, **21**, No. 1, 205–213, doi:10.1109/TMECH.2015.2498169.
24. Tirkolaee E. B., Mardani A., Dashtian Z., Soltani M., Weber G. W., *J. Cleaner Prod.*, 2020, **250**, 119517, doi:10.1016/j.jclepro.2019.119517.
25. Blanco-Mesa F., Merigó J., Gil-Lafuente A. M., *J. Intell. Fuzzy Syst.*, 2017, **32**, No. 3, 2033–2050, doi:10.3233/JIFS-161640.
26. Kalaiarassan G., Somanadh K. M., Thirumalai C., Kumar M. S., *Mater. Today: Proc.*, 2018, **5**, No. 5, 13547–13555, doi:10.1016/j.matpr.2018.02.350.
27. Sáez D., Ávila F., Olivares D., Cañizares C., Marín L., *IEEE Trans. Smart Grid*, 2015, **6**, No. 2, 548–556, doi:10.1109/TSG.2014.2377178.
28. Cheng S. H., Chen S. M., Jian W. S., *Inf. Sci.*, 2016, **327**, 272–287, doi:10.1016/j.ins.2015.08.024.
29. Atsalakis G. S., Atsalaki I. G., Pasiouras F., Zopounidis C., *Eur. J. Oper. Res.*, 2019, **276**, No. 2, 770–780, doi:10.1016/j.ejor.2019.01.040.
30. Kostikova A. V., Tereliansky P. V., Shuvaev A. V., Parakhina V. N., Timoshenko P. N., *ARPN J. Eng. Appl. Sci.*, 2016, **11**, No. 17, 10222–10230, URL http://www.arpnjournals.org/jeas/research_papers/rp_2016/jeas_0916_4906.pdf.
31. Aghbashlo M., Hosseinpour S., Tabatabaei M., Dadak A., *Energy*, 2017, **132**, 65–78, doi:10.1016/j.energy.2017.05.041.
32. Bulut G. G., Güler H., In: *2019 1st Global Power, Energy and Communication Conference (GPECOM)*, IEEE, 2019, 30–34, doi:10.1109/GPECOM.2019.8778568.
33. Chou H. G., Chuang C. F., Wang W. J., Lin J. C., *IEEE Trans. Inf. Forensics Secur.*, 2013, **8**, No. 12, 2177–2185, doi:10.1109/TIFS.2013.2286268.
34. Wang R., Zhang Y., Chen Y., Chen X., Xi L., *Nonlinear Dyn.*, 2020, **100**, 1275–1287, doi:10.1007/s11071-020-05574-x.
35. Kuo C. L., *Int. J. Nonlinear Sci. Numer. Simul.*, 2007, **8**, No. 4, 631–636, doi:10.1515/IJNSNS.2007.8.4.631.
36. Nenciu G., *Int. J. Nonlinear Sci. Numer. Simul.*, 1991, **63**, No. 1, 91, doi:10.1103/RevModPhys.63.91.
37. Buchleitner A., Kolovsky A. R., *Phys. Rev. Lett.*, 2003, **91**, No. 25, 253002, doi:10.1103/PhysRevLett.91.253002.
38. Fallani L., De Sarlo L., Lye J. E., Modugno M., Saers R., Fort C., Inguscio M., *Phys. Rev. Lett.*, 2004, **93**, No. 14, 140406, doi:10.1103/PhysRevLett.93.140406.
39. Denschlag J. H., Simsarian J. E., Häffner H., McKenzie C., Browaeys A., Cho D., Helmerson K., *J. Phys. B: At. Mol. Opt. Phys.*, 2002, **35**, No. 14, 3095–3110, doi:10.1088/0953-4075/35/14/307.
40. Fang J., Hai W., *Physica B*, 2005, **370**, No. 1–4, 61–72, doi:10.1016/j.physb.2005.08.033.
41. Chua V., Porter M. A., *Int. J. Bifurcation Chaos*, 2006, **16**, No. 04, 945–959, doi:10.1142/S0218127406015222.
42. Hai W., Zhu Q., Rong S., *Phys. Rev. A*, 2009, **79**, No. 2, 023603, doi:10.1103/PhysRevA.79.023603.
43. Slotine J. J. E., Li W., *Applied Nonlinear Control*, Prentice Hall International, London, UK, 1991.

Синхронізація хаосу в системі БЕК з використанням нечіткого логічного контролера

Е. Тосіалі¹, Й. Оніз², Ф. Айдогмуз³

¹ Відділення оптики, Професійно-технічне училище охорони здоров'я, Стамбульський університет Білгі, Кустепе, Сіслі, Стамбул, 34387, Туреччина

² Кафедра мехатроніки, Факультет інженерії та природничих наук, Стамбульський університет Білгі, Ейюп, Стамбул, 34060, Туреччина

³ Факультет природничих наук та фізики, Стамбульський університет, Везнечилер, Стамбул, 34134, Туреччина

Оскільки наявність хаосу в Бозе-Ейнштейнівському конденсаті (БЕК) відіграє деструктивну роль та може зменшувати стабільність конденсату, контролювання хаосу має величезне значення для створення БЕК. У цій статті запропонований нечіткий логічний контролер для синхронізації хаотичної динаміки двох ідентичних керуючих рівнянь БЕК систем. На відміну від традиційних підходів, де експертні знання використовуються для отримання правил нечіткого контролю для відповідних функцій, у цій роботі згадані правила побудовані з використанням теореми стійкості Ляпунова для забезпечення процесу синхронізації. Ефективність запропонованого процесу контролю продемонстровано чисельно.

Ключові слова: нечіткий логічний контролер, синхронізація, хаос, Бозе-Ейнштейнівський конденсат